Published in final edited form as:
J Neurooncol. 2006 May ; 78(1): 19–29. doi:10.1007/s11060-005-9068-y.

Reduced glioma infiltration in Src-deficient mice

Caren V. Lund[1,2], **Mai T.N. Nguyen**[1,2], **Geoffrey C. Owens**[1,2], **Andrew J. Pakchoian**[1,2], **Ashkaun Shaterian**[1,2], **Carol A. Kruse**[1,2], and **Brian P. Eliceiri**[1]

[1]Division of Cancer Biology La Jolla Institute for Molecular Medicine, San Diego, CA, 92121, USA

[2]The Neurosciences Institute, 92121, San Diego, CA, USA

Summary

Malignant brain tumors, such as glioblastoma, are characterized by extensive angiogenesis and permeability of the blood-brain barrier (BBB). The infiltration of glioma cells away from the primary tumor mass is a pathological characteristic of glial tumors. The infiltrating tumor cells represent a significant factor in tumor recurrence following surgical debulking, radiation, and chemotherapy treatments. Vascular endothelial growth factor (VEGF)-mediated vascular permeability (VP) has been associated with the progression of glioma tumor growth and infiltration into surrounding normal brain parenchyma. While VEGF induces a robust VP response in control mice ($src^{+/+}$ or $src^{+/-}$), the VP response is blocked in $src^{-/-}$ mice that demonstrate a 'leakage-resistant phenotype' in the brain. We used the Src-deficient mouse model to determine the role of Src in the maintenance of the BBB following orthotopic implantation and growth of glioma cells in the brain. Although solid tumor growth was the same in control and $src^{-/-}$ mice, the infiltrating component of glioma growth was reduced in $src^{-/-}$ mice. Characterization of the expression and localization of the extracellular matrix (ECM) protein fibrinogen was evaluated to determine the effect of a Src-mediated VP defect in the host compartment. These studies indicate that the reduced VP of host brain blood vessels of $src^{-/-}$ mice mediates a reduction in glioma cell invasion in a mouse brain tumor xenograft model.

Keywords

glioblastoma multiforme; glioma invasion; mouse model; vascular permeability; VEGF

Introduction

The blood brain barrier (BBB) is characterized by specialized endothelial cells that form a continuous barrier with low paracellular permeability, ultimately controlling the accessibility of molecules to the brain [1–3]. Tight junctions are a hallmark of the BBB and are formed between endothelial cells in association with other cell types including astrocytes, perivascular macrophages, pericytes, and with the basement membrane [4,5]. Growth of World Health Organization (WHO) grade IV malignant gliomas is associated

Address for offprints: Brian P. Eliceiri, Division of Cancer Biology La Jolla Institute for Molecular Medicine, 4570 Executive Drive, Suite 100, San Diego, CA, 92121, USA; Tel.: +1-858-587-8788; Fax: +1-858-587-6742; beliceiri@ljimm.org.

with changes in the expression and remodeling of perivascular extracellular matrix (ECM) proteins, leading to disruption of the BBB [6–8]. In glioblastoma the compromise of the BBB is associated with increased tumor growth and infiltration [9–12]. Glioma cells are distinct from other tumor cell types in that they rarely metastasize outside of the brain, however, they aggressively invade the surrounding normal brain parenchyma [13–16]. The migration of glioma cells away from the primary tumor mass prevents the complete surgical removal of tumor cells and represents a significant challenge in the treatment of brain tumors [17–22]. For experimental *in vivo* models of brain tumor growth, a significant challenge has been the ability to detect glioma cells infiltrating away from the primary solid tumor [23,24]. Previous studies have demonstrated the applicability of cell-labeling techniques to detect and measure the infiltratation of glioma cells *in vivo* [23,25–28]. A direct comparison between fluorescent microscopy and immunohistochemistry or hematoxylin/eosin staining, has shown that fluorescence or β-galactosidase detection of glioma cells is essential for the detection and characterization of the pathophysiological hallmark of glioma tumor growth, as individual infiltrating glioma cells present in the parenchyma and/or perivascular spaces.

While previous studies have characterized glioma tumor growth, host-mediated mechanisms by which glioma cells migrate and invade the brain is still unclear [29–31]. Like most solid tumors, gliomas express and secrete vascular endothelial growth factor/vascular permeability factor (VEGF/VPF) that induces proliferation and migration of neighboring endothelial cells [32–36]. Remodeling of the BBB vasculature by VEGF disrupts the formation of tight junctions, increases vascular permeability (VP), and results in a disordered vasculature characteristic of tumor-induced angiogenesis [34,37–39]. Our previous studies have demonstrated that the non-receptor tyrosine kinase, Src, is essential for the maintenance of the BBB [40]. VEGF-induced VP of blood vessels of the brain and other organs is reduced in Src-deficient mice. We have shown that Src-deficient mice undergo reduced hematogenous metastasis from the skin to the lung, which is associated with reduced VP and downstream signaling in the blood vessels of the murine host [41]. In this study we examine the consequence of a Src-mediated reduction of tumor-induced permeability of the BBB, an endothelial barrier that is more restrictive than the vascular beds of other organs. While the breakdown of the BBB is associated with the progression of glioma tumors, the capacity for changes in VP to mediate ECM remodeling through hematogenous mechanisms (i.e. perivascular fibrin accumulation) or glioma infiltration through non-hematogenous mechanisms is unknown. Therefore, in this study we have characterized several glioma cell explants at low passage and subsequently implanted them into the brains of Src-deficient ($src^{-/-}$) and control mice ($src^{+/+}$ or $src^{+/-}$) to determine the role of Src in the host compartment during tumor-induced VP, neovascularization, tumor growth, and tumor infiltration in an orthotopic model.

Materials and methods

Src knockout mice

The generation of Src-deficient mice has been previously described [41] and are commercially available back-crossed into the C57BL/6 genetic background (Jackson Labs,

Bar Harbor, ME). For these xenograft studies, the Src-deficient mice have been backcrossed into a Rag2 immunodeficient background [42–44]. Mice were genotyped by PCR analysis for Src and Rag2. All mice were verified to be free of the enteric pathogen *Helicobacter pylori*. All animal studies including surgeries and anesthesia were performed in accordance with institutional animal care and use committee regulations.

Glioma tumor cells

The 02-11-MG (DBTRG) and 13-06-MG glioma cell explants [45] at low passage were used for implantation into $src^{-/-}$ or $src^{+/-}$ mice. Each of these cell explants were derived from patients with grade IV glioblastoma. Their αv integrin expression and ECM interactions have also been assayed ([45] and unpublished observations). Tumor cells were maintained in Dulbecco minimal essential media (Invitrogen, Carlsbad, CA) supplemented with 10% fetal calf serum. Cells were labeled with yellow fluorescent protein (YFP) by transducing them with a lentivirus encoding the YFP gene (LIONII-YFP; kindly provided by Dr. Gary Nolan, Stanford University). Lentiviral particles were generated by transiently transfecting 293T cells with the transfer vector along with plasmids encoding gag/pol and VSV-G envelope genes [46]. Tumor cells were infected *in vitro*, and cells expressing high levels of YFP were isolated by one round of fluorescence-activated cell sorting. Multiple vials of low passage YFP-positive glioma cells (<6 passages) were stored and used for stereotactic brain injection.

Intracranial stereotactic injections

Low passage YFP-labeled 02–11-MG glioma cells were prepared from cell culture at 2×10^8 cells/mL in Hepes-buffered saline. Mice were anesthetized with isoflurane, and after verifying adequate anesthesia, skulls were exposed by a 1 cm longitudinal incision. A burr hole was created 1 mm anterior and 1 mm lateral to the bregma using a hand held drill equipped with a 1/32-inch high-speed cutting bit (Dremel, Racine, WI). Glioma cells, (1×10^6 in 5 μl) were injected into the frontal lobe over 5 min using a microsyringe (Hamilton, Reno, NV) mounted on a stereotactic frame (Kopf Instruments, Tujunga, CA). The incision was closed with veterinary adhesive and topical lidocaine administered. After 21 days, mice were subjected to systemic intracardiac perfusion with heparin-saline, and serial sectioned to yield 1 mm brain slices suitable for *en face* imaging on a glass slide using an Olympus Fluoview 1000 laser scanning confocal microscope (Olympus, Melville, NY). Confocal micrographs in these studies were acquired with 2×/0.08 N.A., 10×/0.4 N.A. or 20×/0.7 N.A. dry objective lenses on a BX61 microscope (Olympus). Quantitation of tumor area in serial brain tumor sections was determined with the image analysis software Volocity (Improvision, Lexington, MA) to measure the sum of pixel values coincident with the YFP-positive tumor area from each of 4–6 brain slices from each of the mice (n=8). A Student t-test was performed to determine the statistical significance of each data set. The legends provide details on the sample size for each analysis.

Immunohistochemistry and VP assay

Indirect immunofluorescence was performed on cryosections (10 μm) of tumor samples using anti-fibrinogen (DAKO, Carpinteria, CA) and anti-CD31 (Becton Dickinson, Franklin

Lakes, NJ) antibodies. The anti-YFP/GFP antibody (A.v., Becton-Dickinson) used detects both GFP and YFP and was used as a complement to the direct imaging of YFP in fresh tissue sections. Alexa fluor-conjugated secondary antibodies were from Molecular Probes (Eugene, OR). The detection of YFP by indirect immunofluorescence in Figures 1b and of YFP and von Willebrand factor (vWF) in the Supplementary data was performed in paraffin sections following antigen retrieval with citrate (pH 6.0, 10 mM) in a pressure cooker. The detection of CD31 and fibrinogen in Figures 3 and 4, respectively were performed in tissue cryosections. Micrographs from random fields within the tumor of control ($src^{+/-}$ or $src^{+/+}$) and $src^{-/-}$ mice from at least 6 separate animals were analyzed. Quantification of fluorescence intensity of CD31 and fibrinogen immunohistochemistry was performed using Volocity to measure fluorescence intensity in blood vessels. The sum of pixel intensities in each fluorescent image field was obtained using matched confocal acquisition settings between Src-knockout and control tissues. The relative image intensity values of CD31 and fibrinogen were measured with a measuring algorithm in Volocity on sections in which the identity was blinded during the analysis. Tumor-induced VP was determined by intravenous injection into the tail vein with 70 kDa rhodamine (TRITC)-dextran (Sigma, St Louis, MO). Fifteen minutes after injection, animals were systemically perfused by intracardiac injection with heparin/saline as previously described [41]. Micrographs were captured from fresh 1 mm brain sections using a confocal microscope to directly detect YFP labeled cells as well as TRITC-dextran, and then subjected to quantitation using the Volocity software as described above.

Immunoblotting

Cell lysates were collected in RIPA buffer (100 mM Tris pH 7.5, 150 mM NaCl, 1 mM EDTA, 1% deoxycholic acid, 1% Triton X-100, 0.1% SDS with freshly added 1 mM orthovanadate, 50 mM NaF, and protease inhibitors cocktail (Roche, Indianapolis, IN). Protein concentration was determined with a BCA Protein Assay (Pierce, Rockford, IL). Twenty micrograms of cell lysate for each sample was separated on a 10% SDS-polyacrylamide gel, transferred to a nitrocellulose membrane, and probed with anti-FAK, anti-Pyk2, or anti-VEGF (Santa Cruz Biotechnologies, Santa Cruz, CA) antibodies. Secondary antibodies were anti-mouse or anti-rabbit antibodies conjugated to horseradish peroxidase. Visualization of antibody binding was detected using Supersignal West Pico Chemiluminescent Substrate (Pierce).

Results

Characterization of chimeric human brain tumor/mouse brain xenograft model

The migratory phenotype of glioma cells into surrounding brain parenchyma is a defining characteristic for malignant gliomas. While the mechanisms regulating glioma tumor invasion are poorly understood, a study of the related tyrosine kinases, Pyk2 and focal adhesion kinase (FAK), in glioma cell migration has shown that elevated Pyk2 expression correlates with increased glioma cell migration *in vitro* [47]. We characterized the expression of FAK, Pyk2, and VEGF (Figure 1a), as well as the expression of various integrins and other signaling intermediates ([45] and data not shown) of two human glioma explants obtained from patients diagnosed with grade IV glioblastoma multiforme (GBM)

[45]. The expression of FAK was similar in both 02-11-MG and 13-06-MG gliomas. In contrast, the expression of Pyk2 was significantly reduced in 13-06-MG glioma cells compared to the 02-11-MG glioma cells. Both glioma cells express VEGF (Figure 1a, bottom row). Based on the correlation of Pyk2 expression and glioma cell migration, and an infiltrative phenotype that has been shown to be characteristic of advanced stage gliomas, we selected 02–11-MG cells to provide a physiologically relevant model of glial tumor growth in a xenograft model of brain tumor growth.

We examined the orthotopic growth of 02-11-MG glioma cells in $src^{-/-}$ vs. control mice ($src^{+/+}$ or $src^{+/-}$). The use of $src^{-/-}$ mice was based on the previously characterized phenotype of $src^{-/-}$ mice that includes reduced blood vessel VP in response to VEGF or tumor-induced VP [40]. Although many parameters influencing glioma growth and infiltration have been previously examined, the role of tumor-induced VP of brain blood vessels had not been examined in a defined genetic model. Therefore, we examined the orthotopic growth of 02-11-MG cells in $src^{-/-}$ and $src^{+/-}$ mice. We have previously shown that $src^{+/+}$ or $src^{+/-}$ have similar VEGF- and tumor-induced responses [41], therefore we have primarily used $src^{+/-}$ mice in our subsequent studies. To facilitate the detection and measurement of glioma tumor growth, 02-11-MG glioma tumor cells were labeled with yellow-fluorescent protein (YFP) (See Materials and methods). Figure 1b demonstrates the invasive behavior of the 02-11 glioma cells following stereotactic injection, 21 day incubation and detection by indirect immunofluorescence with anti-YFP antibody. To compare the tumor burden of 02-11 through multiple brain sections, $src^{-/-}$ and $src^{+/-}$ mice were injected with YFP-labeled 02-11 glioma cells, and following a 21 day incubation, mouse brains were harvested and serial 1 mm sections prepared for image acquisition with a laser scanning confocal microscope (Figure 1c). A representative set of brain slices from $src^{-/-}$ and $src^{+/-}$ mice are shown in Figure 1c. The use of YFP-labeled tumor cells enables the quantitation of tumor burden from the face of each brain slice from each animal. Variation between slices and between animals were averaged to evaluate the tumor volume in $src^{-/-}$ and $src^{+/-}$ mice. The data from tumor volume quantitation is shown in Figure 1d. We determined that there was no significant difference in gross tumor burden between $src^{-/-}$ and $src^{+/-}$ mice. However, when we examined the tumor margin at higher magnification, a Src-mediated effect of the host on tumor infiltration was observed.

Reduced GBM tumor invasion in Src-deficient host mouse brains

Although the gross tumor burden of glioma cells implanted in $src^{-/-}$ and control mice was unchanged (Figure 1d), clinical manifestations of gliomas are associated with the diffuse and infiltrative growth of secondary tumor foci into ipsilateral and contralateral hemispheres [13]. Labeling of glioma tumor cells has been shown to be essential for monitoring the invasion and growth of single glioma cells *in vivo* [23,25–28,48]. Therefore, we examined the growth and invasion of YFP-labeled tumor cells 200–1000 μm from the margin of the primary tumor mass established near the injection site. 02-11-MG glioma tumor cells were injected into the brains of $src^{-/-}$ and $src^{+/-}$ mice, incubated for 21 days, and imaged using standard histological techniques as well as confocal microscopy to detect YFP-labeled cells in fresh brain tissue sections. Hematoxylin/eosin (H/E) staining of sections of tumor-bearing $src^{+/-}$ and $src^{-/-}$ mice suggested that there were differences in the tumor margins between

the host mice (Figure 2a). Arrowheads mark infiltrating tumor cells in $src^{+/-}$ brain sections, whereas, $src^{-/-}$ brain sections had a reduction of infiltrating tumor cells. To more definitively evaluate the extent of glioma cell infiltration, we analyzed YFP-labeled 02-11-MG glioma cells using confocal microscopy. In $src^{+/-}$ mice, 02-11-MG tumor cells exhibited characteristics of grade IV glioma cells with extensive infiltration of the brain parencyhma (arrowheads). However, an examination of the parenchyma of tumor-bearing $src^{-/-}$ mice revealed a decrease in YFP-labeled glioma cell infiltration and formation of infiltrating tumor foci (Figure 2b). We examined the tumor burden from three matched sets of $src^{-/-}$ and $src^{+/-}$ mice and quantitated the number of YFP-positive cells distinct from the primary glioma tumor. Quantitation of these data is presented in Figure 2c, and demonstrates a significant reduction in glioma tumor cell infiltration in $src^{-/-}$ mice (n=8, P<0.05). Therefore, although the gross tumor volume was not reduced in $src^{-/-}$ vs. $src^{+/-}$ mice (Figure 1c), a Src-defect in the host led to a significant reduction in glioma cell infiltration through the brain parenchyma.

$Src^{-/-}$ mice have reduced glioma-induced VP, but normal neovascularization

While glioma growth is associated with increased VP, the mechanism(s) regulating glioma-induced VP remain poorly understood. We have previously shown that VEGF-induced VP is reduced in the brains of Src-deficient mice [40]. Therefore, we examined whether VP induced by a VEGF-expressing glioma tumor would be reduced in the brains of Src-deficient mice. Following the implantation and incubation of 02-11-MG glioma cell in $src^{-/-}$ and $src^{+/-}$ mice, as described above, we injected 70 kDa TRITC-dextran intravenously 15 min before harvest. After systemic intracardiac perfusion to remove intravascular FITC-dextran, we detected FITC-dextran in the perivascular tissue and the YFP-fluorescence in 1 mm brain sections by confocal microscopy immediately upon harvest. Representative micrographs of sibling-matched mice revealed a decrease in 02-11-MG glioma-induced VP in $src^{-/-}$ vs. $src^{+/-}$ mice (Figure 3a). Differences in VP were quantitated and are shown in Figure 3b. Despite the Src-mediated decrease in glioma-induced VP observed in the $src^{-/-}$ brain, neovascularization in response to the brain tumors grown in $src^{-/-}$ and $src^{+/-}$ mice, as monitored by blood vessel staining using anti-CD31 immunofluorescence, was unchanged (Figure 3c). Quantitation of CD31 staining is shown in Figure 3d. These data demonstrate the distinction between tumor-induced VP of the host that is mediated by Src vs. tumor-induced angiogenesis that is independent of a Src defect in the host.

Reduction in tumor-induced fibrinogen accumulation in Src-deficient mice

Endothelial cell migration and increased VP have been associated with remodeling of the ECM and are processes required for tumor progression. The extravasation of plasma fibrinogen, and subsequent cleavage and formation of perivascular fibrin and cross-linked fibrin [collectively referred to as fibrin(-ogen)], are hallmarks of tumor growth [49–51], as well as a pathologically relevant endogenous indicator of VP [41]. Therefore, we examined $src^{-/-}$ and $src^{+/-}$ mice for changes in the distribution of tumor-associated fibrin(-ogen) during glioma growth (Figure 4a). Following implantation and incubation of gliomas in $src^{-/-}$ and $src^{+/-}$ mice, tumor-bearing brains were harvested, cryosectioned, and subjected to immunohistochemical analysis. $Src^{-/-}$ mice showed reduced fibrin(-ogen) staining compared with $src^{+/-}$ mice. The Src-mediated reduction in tumor-associated fibrin was

quantitated from micrographs of fibrin-stained tumor bearing $src^{-/-}$ and $src^{+/-}$ brain sections (Figure 4b). Fibrin(-ogen) associated with CD31-positive blood vessels was also decreased in $src^{-/-}$ mice. These results suggest that reduced accumulation of perivascular fibrin(-ogen) is associated with reduced tumor VP in the brain, and may be an important marker of VP-mediated remodeling of the ECM microenvironment in response to tumor growth.

Discussion

Brain tumors are characterized by an invasive phenotype that prevents complete surgical removal of the tumor mass. Infiltration of glioma cells into normal brain tissue, combined with subsequent tumor growth and increased intracranial pressure, results in a mean survival time of 12–14 months for patients diagnosed with grade IV glioblastoma, the most malignant form of brain tumor [26,52,53]. Recent studies of a cranial tumor model show that increased VP is one of the first events following tumor implantation [54]. Increased VP has been associated with the progression of malignant tumor growth and invasion in the BBB as well as in other tissues, however the molecular basis is unclear. Gliomas express a range of growth factors and cytokines, however VEGF is unique among these growth factors in that it induces VP as well as neovascularization [55–58]. Intra-cranial administration of recombinant VEGF to mice has been shown to increase VP and result in breakdown of the BBB, however the mechanisms regulating this process remain poorly understood [59–61]. Therefore, in this study we have examined Src-deficient mice, which we have previously shown to have a ‘leakage-resistant’ phenotype in response to VEGF. We have used $src^{-/-}$ and $src^{+/-}$ mice to examine the effect of reduced VP of the host vasculature, as well as decreased Src expression in all non-tumor cells, during the growth and infiltration of glioma cells implanted intracranially.

Preventing the infiltration of glioma cells away from the primary tumor is important in any metastasis model. However, the unique environment of the BBB distinguishes glioma growth and infiltration from other models of metastasis in that glioma cells rarely metastasize out of the brain [62], yet are extensively infiltrative within the brain [15]. Our analysis of the growth and infiltration of low passage glioma cells in $src^{-/-}$ mouse brains reveals that the Src-defect of the host can mediate a decrease in glioma cell infiltration of the brain parenchyma, while the overall gross tumor burden and angiogenesis of the primary tumor is unchanged. We have based our studies on the use of low passage glioma cells that exhibit tumor growth and invasion phenotypes similar to infiltrative human gliomas. To evaluate the extent of migration of single or multiple glioma cells away from the primary tumor *in vivo*, glioma cells expressing fluorescent proteins have been shown to provide imaging of glioma cell infiltration [27,28,48]. We show in this work that tumor growth and infiltration can be monitored in serial sections and tumor burden inclusive of solid growth and infiltrative cells can be quantitated to determine gross tumor burden. Furthermore, since we are focused on the role of the host compartment in mediating specific tumor-induced vascular responses (i.e. Src-mediated breakdown of the BBB), the implantation of YFP-labeled tumor cells provides a defined demarcation of tumor cells versus host cells in the xenograft tumor model.

Previous studies have shown that a systemic reduction in VEGF reduces brain tumor growth and infiltration in an orthotopic intracerebral mouse model [63]. However, in contrast to the role of VEGF in both angiogenesis and VP, we have focused on the role of VP, specifically using a Src-knockout model to characterize mechanisms of tumor-induced VP in tumor growth and invasion. While we cannot exclude the possibility that other tumor-expressed factors may induce VP, we have shown that although VEGF-induced VP is blocked in Src-deficient mice, VEGF expression in the brain or fibrinogen expression in the plasma is unchanged in $src^{+/-}$ vs. $src^{-/-}$ mice ([40,60] and data not shown). We propose that the reduction of tumor-induced VP in the brain vascular bed of $src^{-/-}$ mice mediates a reduction in brain tumor infiltration indirectly by regulating the remodeling of the perivascular ECM. For example, fibrin(-ogen) is part of the haemostatic system mediating vascular damage, angiogenesis, and wound repair. In response to VP, plasma fibrinogen undergoes extravasation and cleavage to form perivascular fibrin(-ogen) [50]. Accumulated perivascular fibrin(-ogen) serves as a substrate for endothelial and tumor cell migration and has been associated with tumor extension into normal brain tissue [64–66]. In this study we provide evidence of reduced perivascular fibrin(-ogen) deposition in brain tumor-bearing $src^{-/-}$ mice, suggesting that fibrin(-ogen) may be an example of Src-regulated ECM remodeling that can promote intracranial glioma tumor migration through a VP-dependent mechanism that does not involve the intravasation of tumor cells. Since glioma cells do not infiltrate the brain parenchyma through a hematogenous mechanism, Src-mediated VP may influence the extravasation of plasma fibrinogen, and subsequent cleavage of it to perivascular fibrin(-ogen) to provide a provisional ECM support for glioma cell migration. The observation of the diffuse infiltration of glioma cells is consistent with a model in which a VP defect affects tumor cell invasion, though not necessarily affecting angiogenesis of the primary tumor or satellite tumors.

While *in vitro* studies have shown that Src can regulate many different molecules including intracellular signaling intermediates, integrins, matrix metalloproteases, and ECM proteins, the specific role of Src *in vivo* is poorly understood [67–76]. Based on knockout studies, it is known that other Src-related family kinases can compensate for the absence of Src particularly during development. However, studies have shown that defects in VP cannot be compensated for by other Src family members, and that defects in VP are a phenotype specific for Src-deficient mice [40]. The molecular basis for the role of Src in VEGF-induced VP has been investigated in both brain and lung endothelium and has been shown to require the association of Src with focal adhesion kinase (FAK) [41,77]. However, downstream targets of this Src-mediated signaling pathway have not been identified. Further characterization of the signaling pathway through Src during VEGF-induced VP, or tumor-induced VP, will identify specific mechanisms involved in the process of glioma infiltration in relation to VP. While our previous studies showed that hematogenous metastasis to other organs is reduced in $src^{-/-}$ mice [41], in the brain, the inhibition of tumor-induced VP leads to a change in the perivascular ECM, which may reveal a role for these molecules in mediating the infiltration of brain tumor cells.

Acknowledgments

We thank Mario A. Bourdon and Carole A. Banka for critical reading of this manuscript. Grant support from the NHLBI (B.P.E) and the NINDS (C.A.K.)

Abbreviations

VEGF	vascular endothelial growth factor
VP	vascular permeability
BBB	blood-brain barrier
VEGFR-2	VEGF receptor 2
WHO	World Health Organization
ECM	extracellular matrix

References

1. Ballabh P, Braun A, Nedergaard M. The blood-brain barrier: an overview: structure, regulation, and clinical implications. Neurobiol Dis. 2004; 16:1–13. [PubMed: 15207256]
2. Nag S. Morphology and molecular properties of cellular components of normal cerebral vessels. Methods Mol Med. 2003; 89:3–36. [PubMed: 12958410]
3. Smith QR. A review of blood-brain barrier transport techniques. Methods Mol Med. 2003; 89:193–208. [PubMed: 12958421]
4. Bradbury MW. The blood-brain barrier. Transport across the cerebral endothelium. Circ Res. 1985; 57:213–222. [PubMed: 2410161]
5. Gloor SM, Wachtel M, Bolliger MF, Ishihara H, Landmann R, Frei K. Molecular and cellular permeability control at the blood-brain barrier. Brain Res Brain Res Rev. 2001; 36:258–264. [PubMed: 11690623]
6. Gladson CL. The extracellular matrix of gliomas: modulation of cell function. J Neuropathol Exp Neurol. 1999; 58:1029–1040. [PubMed: 10515226]
7. Mahesparan R, Read TA, Lund-Johansen M, Skaftnesmo KO, Bjerkvig R, Engebraaten O. Expression of extracellular matrix components in a highly infiltrative in vivo glioma model. Acta Neuropathol (Berl). 2003; 105:49–57. [PubMed: 12471461]
8. Davies DC. Blood-brain barrier breakdown in septic encephalopathy and brain tumours. J Anat. 2002; 200:639–646. [PubMed: 12162731]
9. Coomber BL, Stewart PA, Hayakawa K, Farrell CL, Del Maestro RF. Quantitative morphology of human glioblastoma multiforme microvessels: structural basis of blood-brain barrier defect. J Neurooncol. 1987; 5:299–307. [PubMed: 2831312]
10. Nag S. Pathophysiology of blood-brain barrier breakdown. Methods Mol Med. 2003; 89:97–119. [PubMed: 12958415]
11. Oliveira R, Christov C, Guillamo JS, Debouard S, Palfi S, Venance L, Tardy M, Peschanski M. Contribution of gap junctional communication between tumor cells and astroglia to the invasion of the brain parenchyma by human glioblastomas. BMC Cell Biol. 2005; 6:7. [PubMed: 15715906]
12. Henson JW, Gaviani P, Gonzalez RG. MRI in treatment of adult gliomas. Lancet Oncol. 2005; 6:167–175. [PubMed: 15737833]
13. Demuth T, Berens ME. Molecular mechanisms of glioma cell migration and invasion. J Neurooncol. 2004; 70:217–228. [PubMed: 15674479]
14. Giese A, Bjerkvig R, Berens ME, Westphal M. Cost of migration: invasion of malignant gliomas and implications for treatment. J Clin Oncol. 2003; 21:1624–1636. [PubMed: 12697889]

15. Mourad PD, Farrell L, Stamps LD, Chicoine MR, Silbergeld DL. Why are systemic glioblastoma metastases rare? Systemic and cerebral growth of mouse glioblastoma. Surg Neurol. 2005; 63:511–519. discussion 519. [PubMed: 15936366]
16. Bolteus AJ, Berens ME, Pilkington GJ. Migration and invasion in brain neoplasms. Curr Neurol Neurosci Rep. 2001; 1:225–232. [PubMed: 11898522]
17. Bellail AC, Hunter SB, Brat DJ, Tan C, Van Meir EG. Microregional extracellular matrix heterogeneity in brain modulates glioma cell invasion. Int J Biochem Cell Biol. 2004; 36:1046–1069. [PubMed: 15094120]
18. Desjardins A, Rich JN, Quinn JA, Vredenburgh J, Gururangan S, Sathornsumetee S, Reardon DA, Friedman AH, Bigner DD, Friedman HS. Chemotherapy and novel therapeutic approaches in malignant glioma. Front Biosci. 2005; 10:2645–2668. [PubMed: 15970525]
19. Fujimaki T. Surgical treatment of brain metastasis. Int J Clin Oncol. 2005; 10:74–80. [PubMed: 15864691]
20. Gilbert MR, Loghin M. The Treatment of Malignant Gliomas. Curr Treat Options Neurol. 2005; 7:293–303. [PubMed: 15967092]
21. Nabors LB, Fiveash J. Treatment of adults with recurrent malignant glioma. Expert Rev Neurother. 2005; 5:509–514. [PubMed: 16026234]
22. Berens ME, Giese A. "…those left behind." Biology and oncology of invasive glioma cells. Neoplasia. 1999; 1:208–219. [PubMed: 10935475]
23. Lampson LA, Lampson MA, Dunne AD. Exploiting the lacZ reporter gene for quantitative analysis of disseminated tumor growth within the brain: use of the lacZ gene product as a tumor antigen, for evaluation of antigenic modulation, and to facilitate image analysis of tumor growth in situ. Cancer Res. 1993; 53:176–182. [PubMed: 8416743]
24. Owens GC, Orr EA, DeMasters BK, Muschel RJ, Berens ME, Kruse CA. Overexpression of a transmembrane isoform of neural cell adhesion molecule alters the invasiveness of rat CNS-1 glioma. Cancer Res. 1998; 58:2020–2028. [PubMed: 9581848]
25. Pedersen PH, Edvardsen K, Garcia-Cabrera I, Mahesparan R, Thorsen J, Mathisen B, Rosenblum ML, Bjerkvig R. Migratory patterns of lac-z transfected human glioma cells in the rat brain. Int J Cancer. 1995; 62:767–771. [PubMed: 7558428]
26. Prados MD, Berger MS, Wilson CB. Primary central nervous system tumors: advances in knowledge and treatment. CA Cancer J Clin. 1998; 48:331–360. 321. [PubMed: 9838898]
27. MacDonald TJ, Tabrizi P, Shimada H, Zlokovic BV, Laug WE. Detection of brain tumor invasion and micrometastasis in vivo by expression of enhanced green fluorescent protein. Neurosurgery. 1433; 43:1437–1442. [PubMed: 9848858]
28. Mourad PD, Farrell L, Stamps LD, Santiago P, Fillmore HL, Broaddus WC, Silbergeld DL. Quantitative assessment of glioblastoma invasion in vivo. Cancer Lett. 2003; 192:97–107. [PubMed: 12637158]
29. Bello L, Giussani C, Carrabba G, Pluderi M, Costa F, Bikfalvi A. Angiogenesis and invasion in gliomas. Cancer Treat Res. 2004; 117:263–284. [PubMed: 15015565]
30. Tonn JC, Goldbrunner R. Mechanisms of glioma cell invasion. Acta Neurochir Suppl. 2003; 88:163–167. [PubMed: 14531574]
31. Lefranc F, Brotchi J, Kiss R. Possible future issues in the treatment of glioblastomas: special emphasis on cell migration and the resistance of migrating glioblastoma cells to apoptosis. J Clin Oncol. 2005; 23:2411–2422. [PubMed: 15800333]
32. Jensen RL. Growth factor-mediated angiogenesis in the malignant progression of glial tumors: a review. Surg Neurol. 1998; 49:189–195. discussion 196. [PubMed: 9457270]
33. Berkman RA, Merrill MJ, Reinhold WC, Monacci WT, Saxena A, Clark WC, Robertson JT, Ali IU, Oldfield EH. Expression of the vascular permeability factor/vascular endothelial growth factor gene in central nervous system neoplasms. J Clin Invest. 1993; 91:153–159. [PubMed: 8380810]
34. Machein MR, Plate KH. VEGF in brain tumors. J Neurooncol. 2000; 50:109–120. [PubMed: 11245271]
35. Ferrara N, Gerber HP, LeCouter J. The biology of VEGF and its receptors. Nat Med. 2003; 9:669–676. [PubMed: 12778165]

36. Autiero M, Waltenberger J, Communi D, Kranz A, Moons L, Lambrechts D, Kroll J, Plaisance S, De Mol M, Bono F, et al. Role of PlGF in the intra- and intermolecular cross talk between the VEGF receptors Flt1 and Flk1. Nat Med. 2003; 9:936–943. [PubMed: 12796773]
37. Vaquero J, Zurita M, Morales C, Cincu R, Oya S. Expression of vascular permeability factor in glioblastoma specimens: correlation with tumor vascular endothelial surface and peritumoral edema. J Neurooncol. 2000; 49:49–55. [PubMed: 11131986]
38. Harhaj NS, Antonetti DA. Regulation of tight junctions and loss of barrier function in pathophysiology. Int J Biochem Cell Biol. 2004; 36:1206–1237. [PubMed: 15109567]
39. Schneider SW, Ludwig T, Tatenhorst L, Braune S, Oberleithner H, Senner V, Paulus W. Glioblastoma cells release factors that disrupt blood-brain barrier features. Acta Neuropathol (Berl). 2004; 107:272–276. [PubMed: 14730455]
40. Eliceiri BP, Paul R, Schwartzberg PL, Hood JD, Leng J, Cheresh DA. Selective requirement for Src kinases during VEGF-induced angiogenesis and vascular permeability. Mol Cell. 1999; 4:915–924. [PubMed: 10635317]
41. Criscuoli ML, Nguyen M, Eliceiri BP. Tumor metastasis but not tumor growth is dependent on Src-mediated vascular permeability. Blood. 2005; 105:1508–1514. [PubMed: 15486073]
42. Chen J, Lansford R, Stewart V, Young F, Alt FW. RAG-2-deficient blastocyst complementation: an assay of gene function in lymphocyte development. Proc Natl Acad Sci U S A. 1993; 90:4528–4532. [PubMed: 8506294]
43. Hochedlinger K, Blelloch R, Brennan C, Yamada Y, Kim M, Chin L, Jaenisch R. Reprogramming of a melanoma genome by nuclear transplantation. Genes Dev. 2004; 18:1875–1885. [PubMed: 15289459]
44. Mazurier F, Fontanellas A, Salesse S, Taine L, Landriau S, Moreau-Gaudry F, Reiffers J, Peault B, Di Santo JP, de Verneuil H. A novel immunodeficient mouse model – RAG2 x common cytokine receptor gamma chain double mutants – requiring exogenous cytokine administration for human hematopoietic stem cell engraftment. J Interferon Cytokine Res. 1999; 19:533–541. [PubMed: 10386866]
45. Mattern RH, Read SH, Pierschbacher MD, Sze CI, Eliceiri B, Kruse CA. Glioma cell integrin expression and their interactions with integrin antagonists. Cancer Therapy. 2005; 3:325–340. [PubMed: 16467916]
46. Curran MA, Kaiser SM, Achacoso PL, Nolan GP. Efficient transduction of nondividing cells by optimized feline immunodeficiency virus vectors. Mol Ther. 2000; 1:31–38. [PubMed: 10933909]
47. Lipinski CA, Tran NL, Menashi E, Rohl C, Kloss J, Bay RC, Berens ME, Loftus JC. The tyrosine kinase pyk2 promotes migration and invasion of glioma cells. Neoplasia. 2005; 7:435–445. [PubMed: 15967096]
48. Zhang X, Li X, Wu JW, Gao DK, Liang JW, Liu XZ. Experiment and observation on invasion of brain glioma in vivo. J Clin Neurosci. 2002; 9:668–671. [PubMed: 12604281]
49. Degen JL, Palumbo JS. Mechanisms linking hemostatic factors to tumor growth in mice. Pathophysiol Haemost Thromb. 2003; 33(Suppl 1):31–35. [PubMed: 12954998]
50. Staton CA, Brown NJ, Lewis CE. The role of fibrinogen and related fragments in tumour angiogenesis and metastasis. Expert Opin Biol Ther. 2003; 3:1105–1120. [PubMed: 14519075]
51. Wojtukiewicz MZ, Sierko E, Rak J. Contribution of the hemostatic system to angiogenesis in cancer. Semin Thromb Hemost. 2004; 30:5–20. [PubMed: 15034794]
52. Stupp R, van den Bent MJ, Hegi ME. Optimal role of temozolomide in the treatment of malignant gliomas. Curr Neurol Neurosci Rep. 2005; 5:198–206. [PubMed: 15865885]
53. Thorsen F, Tysnes BB. Brain tumor cell invasion, anatomical and biological considerations. Anticancer Res. 1997; 17:4121–4126. [PubMed: 9428345]
54. Hansen-Algenstaedt N, Joscheck C, Schaefer C, Lamszus K, Wolfram L, Biermann T, Algenstaedt P, Brockmann MA, Heintz C, Fiedler W, et al. Long-term observation reveals time-course-dependent characteristics of tumour vascularisation. Eur J Cancer. 2005; 41:1073–1085. [PubMed: 15862758]
55. Brockmann MA, Ulbricht U, Gruner K, Fillbrandt R, Westphal M, Lamszus K. Glioblastoma and cerebral microvascular endothelial cell migration in response to tumor-associated growth factors. Neurosurgery. 1399; 52:1391–1399. [PubMed: 12762884]

56. Kaur B, Tan C, Brat DJ, Post DE, Van Meir EG. Genetic and hypoxic regulation of angiogenesis in gliomas. J Neurooncol. 2004; 70:229–243. [PubMed: 15674480]
57. Lamszus K, Heese O, Westphal M. Angiogenesis-related growth factors in brain tumors. Cancer Treat Res. 2004; 117:169–190. [PubMed: 15015561]
58. Dunn IF, Heese O, Black PM. Growth factors in glioma angiogenesis: FGFs, PDGF, EGF, and TGFs. J Neurooncol. 2000; 50:121–137. [PubMed: 11245272]
59. Zhang ZG, Zhang L, Jiang Q, Zhang R, Davies K, Powers C, Bruggen N, Chopp M. VEGF enhances angiogenesis and promotes blood–brain barrier leakage in the ischemic brain. J Clin Invest. 2000; 106:829–838. [PubMed: 11018070]
60. Paul R, Zhang ZG, Eliceiri BP, Jiang Q, Boccia AD, Zhang RL, Chopp M, Cheresh DA. Src deficiency or blockade of Src activity in mice provides cerebral protection following stroke. Nat Med. 2001; 7:222–227. [PubMed: 11175854]
61. Zhang ZG, Zhang L, Tsang W, Soltanian-Zadeh H, Morris D, Zhang R, Goussev A, Powers C, Yeich T, Chopp M. Correlation of VEGF and angiopoietin expression with disruption of blood-brain barrier and angiogenesis after focal cerebral ischemia. J Cereb Blood Flow Metab. 2002; 22:379–392. [PubMed: 11919509]
62. Armanios MY, Grossman SA, Yang SC, White B, Perry A, Burger PC, Orens JB. Transmission of glioblastoma multiforme following bilateral lung transplantation from an affected donor: case study and review of the literature. Neurooncol. 2004; 6:259–263.
63. Kunkel P, Ulbricht U, Bohlen P, Brockmann MA, Fillbrandt R, Stavrou D, Westphal M, Lamszus K. Inhibition of glioma angiogenesis and growth in vivo by systemic treatment with a monoclonal antibody against vascular endothelial growth factor receptor-2. Cancer Res. 2001; 61:6624–6628. [PubMed: 11559524]
64. Bardos H, Molnar P, Csecsei G, Adany R. Fibrin deposition in primary and metastatic human brain tumours. Blood Coagul Fibrinolysis. 1996; 7:536–548. [PubMed: 8874864]
65. Yumitori K, Handa H, Teraura T, Yamashita J, Yamamura K. Metastatic brain tumour and fibrinopeptides. Acta Neurochir (Wien). 1987; 89:43–47. [PubMed: 3434341]
66. Sawaya R, Mandybur T, Ormsby I, Tew JM, Westhoff MA, Serrels B, Fincham VJ, Frame MC, Carragher NO. SRC-mediated phosphorylation of focal adhesion kinase couples actin and adhesion dynamics to survival signaling. Mol Cell Biol. 2004; 24:8113–8133. [PubMed: 15340073]
68. Campbell ID. Modular proteins at the cell surface. Biochem Soc Trans. 2003; 31:1107–1114. [PubMed: 14641006]
69. Shattil SJ. Integrins and Src: dynamic duo of adhesion signaling. Trends Cell Biol. 2005; 15:399–403. [PubMed: 16005629]
70. Courter DL, Lomas L, Scatena M, Giachelli CM. Src kinase activity is required for integrin alphaVbeta3-mediated activation of nuclear factor-kappaB. J Biol Chem. 2005; 280:12145–12151. [PubMed: 15695822]
71. Playford MP, Schaller MD. The interplay between Src and integrins in normal and tumor biology. Oncogene. 2004; 23:7928–7946. [PubMed: 15489911]
72. Wu X, Gan B, Yoo Y, Guan JL. FAK-Mediated Src Phosphorylation of Endophilin A2 Inhibits Endocytosis of MT1-MMP and Promotes ECM Degradation. Dev Cell. 2005; 9:185–196. [PubMed: 16054026]
73. Labrecque L, Nyalendo C, Langlois S, Durocher Y, Roghi C, Murphy G, Gingras D, Beliveau R. Src-mediated tyrosine phosphorylation of caveolin-1 induces its association with membrane type 1 matrix metalloproteinase. J Biol Chem. 2004; 279:52132–52140. [PubMed: 15466865]
74. Sounni NE, Roghi C, Chabottaux V, Janssen M, Munaut C, Maquoi E, Galvez BG, Gilles C, Frankenne F, Murphy G, et al. Up-regulation of vascular endothelial growth factor-A by active membrane-type 1 matrix metalloproteinase through activation of Src-tyrosine kinases. J Biol Chem. 2004; 279:13564–13574. [PubMed: 14729679]
75. Nadav L, Katz BZ. The molecular effects of oncogenesis on cell-extracellular matrix adhesion (review). Int J Oncol. 2001; 19:237–246. [PubMed: 11445834]
76. Yang Y, Dang D, Mogi S, Ramos DM. Tenascin-C deposition requires beta3 integrin and Src. Biochem Biophys Res Commun. 2004; 322:935–942. [PubMed: 15336554]

77. Eliceiri BP, Puente XS, Hood JD, Stupack DG, Schlaepfer DD, Huang XZ, Sheppard D, Cheresh DA. Src-mediated coupling of focal adhesion kinase to integrin alpha(v)beta5 in vascular endothelial growth factor signaling. J Cell Biol. 2002; 157:149–160. [PubMed: 11927607]

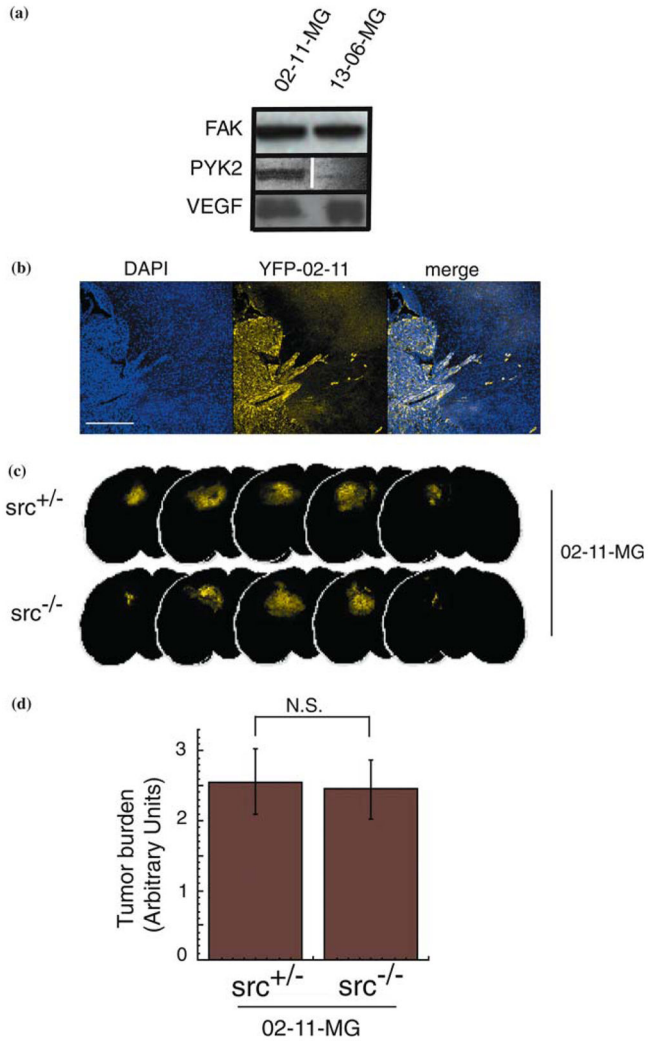

Figure 1.

Characterization of Pyk2 and FAK expression by glioma cells *in vitro* and *in vivo*. (a) Lysates of cultured low passage glial cells, 02-11- MG and 13-06-MG, were prepared as described in the Materials and Methods and subjected to immunoblotting with anti-Pyk2, anti-FAK and anti-VEGF antibodies. Protein-antibody complexes were detected using ECL detection. (b) Infiltration of yellow fluorescent protein (YFP)- labeled 02-11-MG tumor cells was examined in the fixed brain sections by indirect immunofluorescence with an anti-YFP/GFP antibody (middle panel). DAPI staining labels nuclei (left panel) and a merge of the nuclei and tumor cells is also shown (right panel). Bar=200 μm. (c) Fluorescent micrographs embedded in illustrated serial brain sections from mice bearing YFP-labeled 02-11-MG tumor cells, with $src^{+/-}$ sections in the top row and $src^{-/-}$ sections in the bottom row. Tumors were stereotactically injected and allowed to grow for 21 days. Upon harvest, brains were sectioned and images of unfixed serial sections were acquired with a laser scanning confocal microscope. (d) Tumor volume was calculated for 02- 11-MG tumors in $src^{+/-}$ and $src^{-/-}$ brain sections. Tumor area was quantitated by imaging the faces of serial 1.0 mm brain slices from sibling-matched mice (n=8).

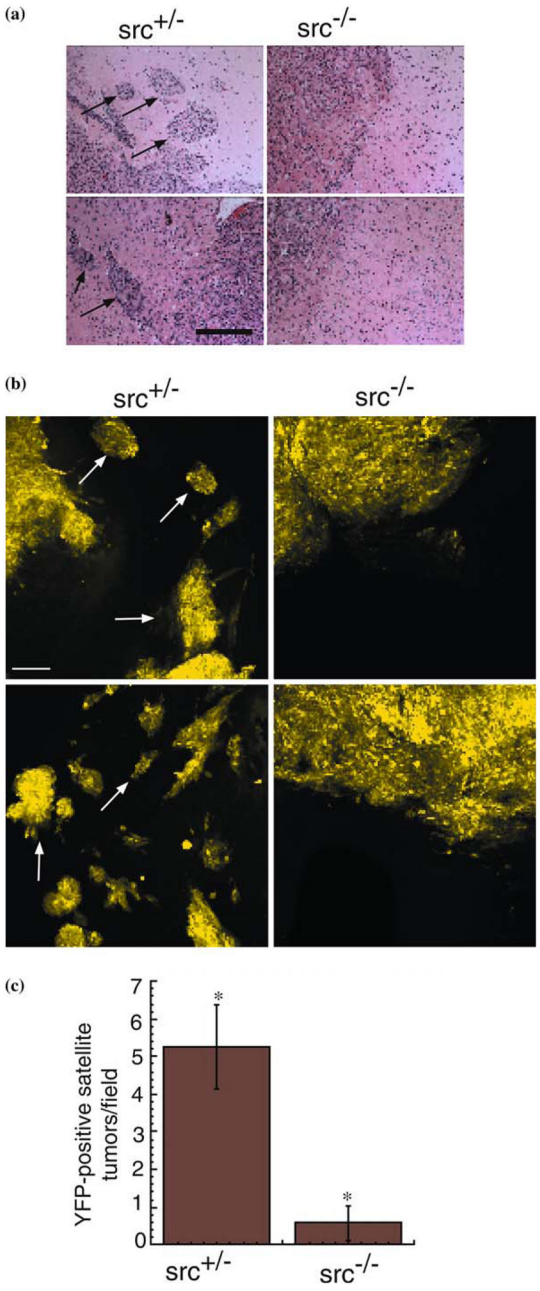

Figure 2.

Reduced perivascular extension of 02-11-MG glioma cells into $src^{+/-}$ vs. $src^{-/-}$ mouse brains. (a) Low power photomicrographs from hematoxylin/eosin stained brain tumor sections at the boundary of 02-11-MG tumor growth in representative brain section from $src^{+/-}$(left panel) and $src^{-/-}$(right panel) mice. Arrows indicate perivascular tumor foci. Bar=200μm. (b) Confocal micrographs at 20× of $src^{+/-}$ and $src^{-/-}$ mice bearing YFP-labeled 02-11-MG with tumor foci indicated with arrows. The left two panels are representative images of $src^{+/-}$ brain sections and the right two panels are representative of $src^{-/-}$ brain sections. Arrows indicate tumor foci. Micrographs were imaged at a distance of 200–1000 μm from the primary solid tumor margin. Bar=200 μm. (c) Quantitation of tumor foci observed in $src^{+/-}$ and $src^{-/-}$ mice. Asterisks indicate a statistically significant difference (n=8, P<0.05).

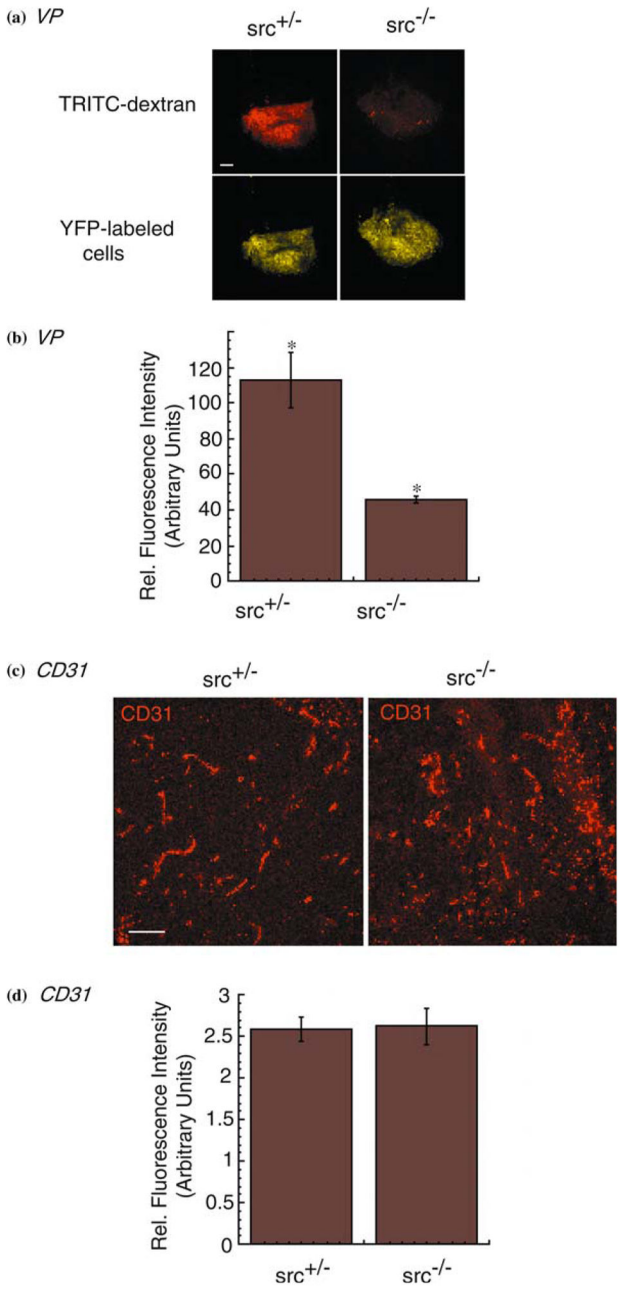

Figure 3.

Reduction of tumor-induced VP but not angiogenesis in Src-knockout mice. (a) Tumor-induced VP was determined in $src^{+/-}$(top left panel) and $src^{-/-}$(top right panel) mice bearing intracranial 02-11-MG tumor cells using extravasation of TRITC-70 kDa dextran. YFP-labeled brain tumor burden in $src^{+/-}$(bottom left panel) and $src^{-/-}$(bottom right panel) mice was obtained by imaging with a confocal microscope as described in the Materials and Methods. Mice were subjected to intravenous injection of TRITC-70 kDa dextran, perfused with heparin/saline to remove intravascular dextran, and the harvested brains subjected to serial 1 mm sectioning and imaging. Micrographs were imaged at 2× and dextran fluorescence detected. Bar= 1000 μm. (b) Quantitation of VP as detected by fluorescence of TRITC-70 kDa dextran as described in the Materials and Methods. (n=6; P<0.05). (c) Indirect immunofluorescence of cryosections from cranial 02-11-MG tumors grown in $src^{+/-}$(left panel) and

src$^{-/-}$(right panel) mice. Immunostaining with an anti-CD31 antibody was used to localize blood vessels in the tumor. Bar=100 μm. (d) Quantitation of CD31 staining as described in the Materials and methods. (n=6).

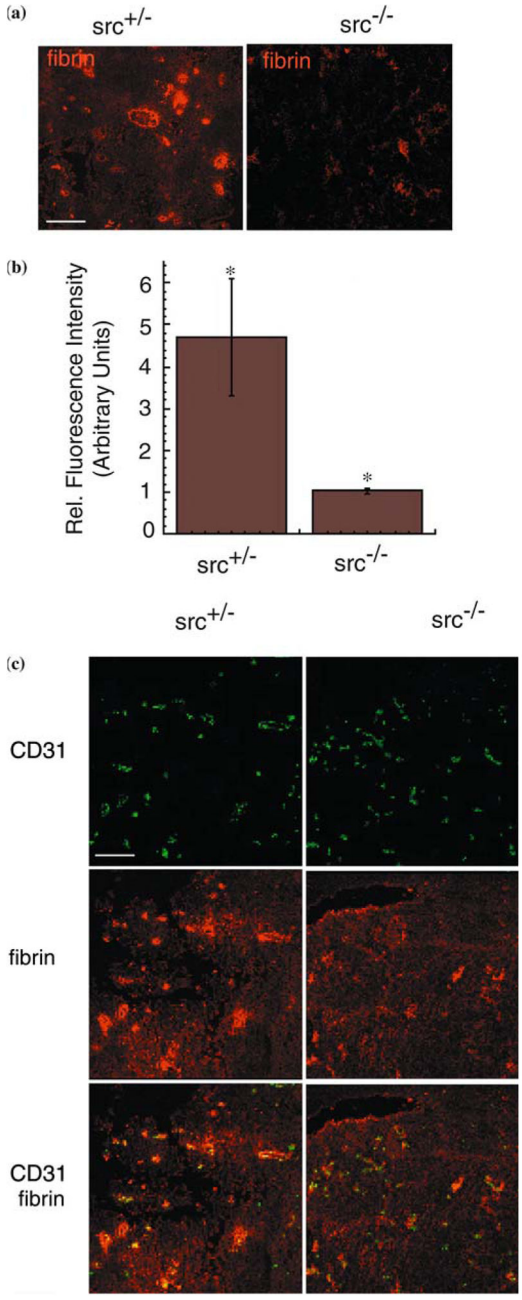

Figure 4.

Reduced colocalization of perivascular fibrin and CD31 staining in tumor-bearing $src^{-/-}$ mouse brains. (a) Indirect immunofluorescence of cryosections of 02-11-MG tumor-bearing $src^{+/-}$(left) and $src^{-/-}$ brains (right) immunostained with an anti-fibrin(- ogen) antibody. Bar = 100 μm. (b) Quantitation of fibrinogen immunostaining in 02-11-MG tumor-bearing $src^{+/-}$ and $src^{-/-}$ brains, as described in the Materials and methods. (n=6, P<0.05). (c) Localization of CD31-positive blood vessels and fibrin(-ogen) in 02-11-MG tumor-bearing $src^{+/-}$(left) and $src^{-/-}$ brains (right). Bar = 100 μm.